A study of stability effects in forested terrain

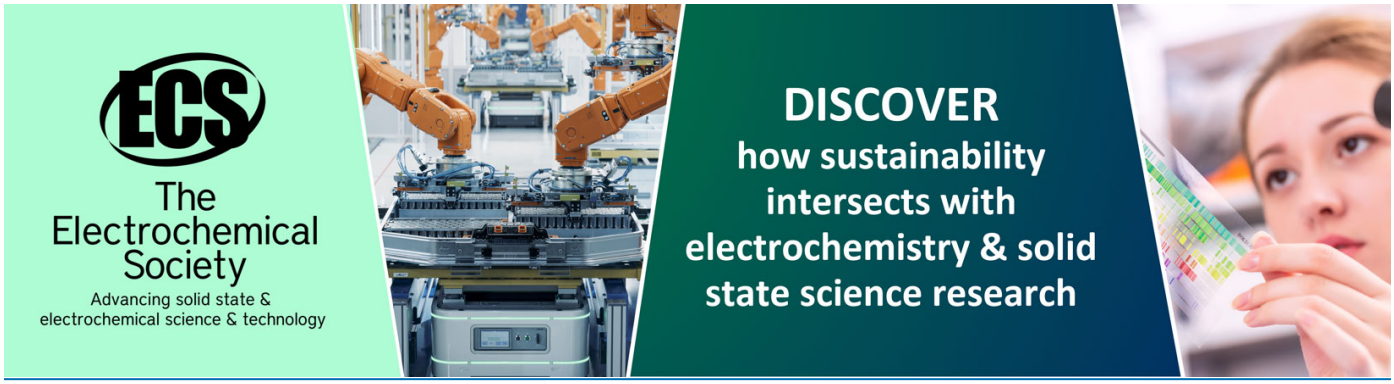

A study of stability effects in forested terrain

Cian J Desmond[1], Simon Watson
CREST, School of Electronic and Electrical Engineering, *Loughborough University*, Holywell Park, Loughborough, Leicestershire LE11 3TU
E-mail: cian.desmond@dnvgl.com

Abstract. Data from four well instrumented met masts located in heavily forested European sites in different locations and terrain types are examined. Seven stability metrics are applied to the data sets and a novel method is used to identify the metric which most consistently identifies stability events of importance for wind energy generation. It was found that the Obukhov length, as calculated by fast response sonic anemometer, provides the most reliable results in these highly complex sites. It was also found that non-neutral stabilities can be expected a significant portion of the time for wind speeds of less than 10 m/s at the considered sites.

1. Introduction

Complex sites pose a significant challenge for the development of wind farms due to unpredictable flow patterns and increased levels of turbulence. In this era of financial rigor it is important to be able to understand these flows and their effect both on the energy capture and fatiguing of wind turbines.

Forestry is a particular form of complex terrain in which wind farms are now being increasingly developed. To date, it has been common to use linearised flow models along with empirical and experience led corrections when predicting wind characteristics in such areas. More recently, the use of full computational fluid dynamics (CFD) solvers has become common. Whilst satisfactory results have been achieved using these codes, simulations are predominately limited to neutral atmospheric stabilities.

The evolution of stability effects within the atmospheric boundary layer is an intricate process which depends on many factors such as wind shear, ambient turbulence levels, wind speeds, the Coriolis Effect, potential temperature gradients and vertical heat fluxes. Certain surface features present in complex terrain can severely alter some of these factors making it difficult to assess stability effects.

For example, local thermal stratification can be significantly affected by forests as they act as large thermal masses which are slow to heat up and cool down as solar irradiance levels vary. Also, depending on the density of the canopy, forests act as a buffer between the underlying soil and the atmosphere which inhibits surface heat flux[1]. These factors result in characteristic thermal stratifications within and above forests which vary significantly over the diurnal cycle. Generalised profiles are displayed in Figure 1 which shows how mean potential temperature, $\bar{\theta}$, and vertical heat flux, $\overline{\omega'\theta'}$, vary throughout the canopy height. Values are normalised to values at the top of the canopy, h_c.

[1]To whom any correspondence should be addressed.

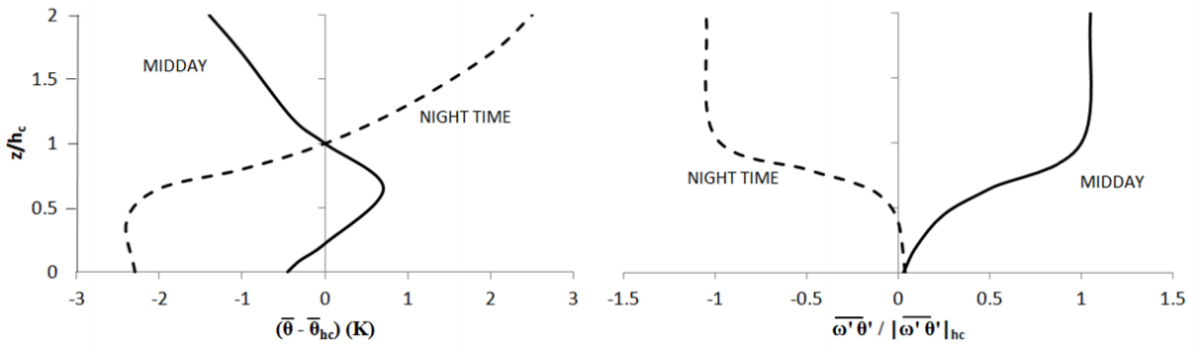

Figure 1. Typical mean potential temperature and vertical heat flux profiles in and above a forest canopy for midday and night time conditions. Reproduced from [2]

It has also been established that forests have a profound effect on both wind shear and ambient turbulence levels above and downstream of canopies [3]. The aggregated effect of these factors is an extremely complicated atmosphere in the vicinity of forests which makes the assessment of stability a non trivial task. However, it is important that we arrive at a satisfactory quantifiable measure as stability effects heavily influence how the wind interacts with the surface features present in such complex terrain [4,5].

Data sets are examined from four forested sites in various terrains and geographical locations. Seven stability metrics, which have been developed for various purposes, are investigated. The metric that consistently differentiates between stable and unstable events of consequence to wind energy generation is identified, critical values are established and the implications are briefly discussed.

2. Stability metrics

As mentioned above, the evolution of stability effects within the atmospheric boundary layer is a complex process caused by many factors, an excellent introduction to which can be found in [6]. Here we will limit the discussion to a brief introduction to the metrics that have been devised to quantify stability effects.

2.1. Richardson Number

Denoted as, *Ri*, this is a non-dimensional parameter which relates the importance of buoyancy and shear forces in creating turbulence. It requires measurements of both temperature and wind speed at two heights and is given by the equation below[2].

$$Ri = \frac{g}{\bar{\theta}}\left[\frac{\partial\bar{\theta}/\partial z}{(\partial\bar{U}/\partial z)^2}\right]$$

Where,

g	=	*9.81 m/s ,*
$\bar{\theta}$	=	Average potential temperature *(K)*
$\partial\bar{\theta}/\partial z$	=	rate of change of potential temperature with height *(K/m)*

The Richardson number is thus positive for stable atmospheric stratification, negative for unstable and zero for neutral. Near-neutral conditions can be assumed [9] for values of:

$$-0.13 \leq Ri \leq 0.03$$

2.2. Bulk Richardson Number

This modified version of *Ri* appears in a variety of forms, such as [7]:

$$Ri_b = \frac{g}{\bar{\theta}_2}.z_2.\left[\frac{\Delta\bar{\theta}}{\overline{U}_2^2}\right]$$

The symbols have the same interpretation as above with the subscript "$_2$" referring to the higher measurement point. This metric again requires temperature measurements at two heights but only a single wind speed.

2.3. Richardson Bulk Number in Forestry

This is a form of Ri_b which was devised specifically for investigating vertical mixing above forest due to stability effects [8]. It will be referred to in this paper as Ri_{b2}:

$$Ri_{b2} = \frac{1}{\overline{U}_2^2}.\frac{g}{\bar{\theta}_2}.\Delta\bar{\theta}\Delta z$$

Compared to Ri_b the main difference with this metric is that the higher measurements are taken above the canopy and the lower temperature measurement within the canopy at a height of 1-2 m above the ground.

2.4. Obukhov Length

This is another important metric for the assessment of stability in the atmospheric boundary layer and is calculated from the equation [6]:

$$\frac{1}{L} = -\frac{\kappa.\left(\frac{g}{\bar{\theta}}\right).\left(\overline{\omega'\theta'}\right)}{U_*}$$

Where, κ = Von Kármán constant = *0.41*
$\left(\overline{\omega'\theta'}\right)$ = Average vertical heat flux *(K m/s)*
U_* = Friction velocity (m/s)

And,

$$U_* = \left[\left(\overline{u'\omega'}\right)^2 + \left(\overline{v'\omega'}\right)^2\right]^{0.25}$$

Where, u', v', ω' = Wind velocity turbulent fluctuations in x , y , z (m/s)
$\left(\overline{u'\omega'}\right)$ = Covariance of both parameters *(m^2/s^2)*

Conventionally, the Obukhov length has units of metres and can be taken as the depth of the mechanically mixed portion of the boundary layer. $1/L$ will be positive in stable conditions and negative in unstable. The following values are expected for near-neutral stability [22]:

$$-0.005 \leq \frac{1}{L} \leq 0.005$$

2.5. *Kazanski-Monin parameter*
This is a slight variation on the Obukhov Lengh which includes the effect of the Coriolis parameter. It was devised for estimating the rate of plume growth for dispersion modelling and is given by the following equation [23]:

$$\mu = \frac{\kappa U_*}{fL}$$

Where, *f,* is the Coriolis parameter:

$$f = 2\Omega \sin \phi$$

Where, ϕ, is the latitude of the measurement location and Ω is the rotational velocity of the Earth which is approximately:

$$\Omega = 7.2921\ x\ 10^{-5}\ rad/sec$$

2.6. Environmental Stability Parameter
This parameter focuses only on the potential temperature gradient [9]:

$$S = \frac{g}{\bar{\theta}} . \frac{d\bar{\theta}}{dz}$$

This parameter has units of s^{-2} and is proportional to the rate at which the generation of turbulence is suppressed. Positive values are indicative of stable conditions; negative of unstable with values close to zero expected for near-neutral conditions.

2.7. Standard Deviation of Direction
This measure was by proposed by the US Nuclear Regulation Commission [10] to assess atmospheric stability for the purposes of guiding emergency responses in the event of an incident. A high value of the standard deviation of wind direction turbulent fluctuations, σ_φ, indicates unstable conditions; low values indicate stable conditions and near-neutral conditions are characterised by some intermediate value. Specific values will be highly site and measurement height dependant. For the purposes of comparison with the other metrics the inverse of this term, $1/\sigma_\varphi$, will be used

3. Site data
Data have been collected from four separate met masts located in forested terrain for the purposes of this analysis.

3.1 Norunda
This mast is located in the middle of a heavily forested area in Sweden (60° 5' N , 17° 28' E) and was established for the purposes of studying fluxes of CO_2. The mast is located in flat terrain in the middle of a dense coniferous forest with a mean canopy height of 30m. Data were available in 30 min averages for the period 7/7/06 – 18/09/06 from a 100 m met mast recorded by a series of sonic anemometers (Metek USA-1) and temperature sensors. Concurrent solar irradiance data were also available from a pyranometer located at the top of the mast. This is a relatively short measurement period; however, the variation in irradiance levels experienced provides sufficient data for our purposes. For additional information on the instrumentation please refer to [11].

It was possible to calculate values for all of the stability metrics discussed above at heights between 28m – 36.9 m. Values of shear exponent α at 87m and turbulent kinetic energy (*TKE*) at 31.8m were calculated as the parameters of interest for the purpose of resource assessment using the equations below:

$$\alpha = \log(\overline{U}_2 / \overline{U}_1)/\log(z_2/z_1) \qquad TKE = \frac{1}{2}\,(\sigma_u^2 + \sigma_v^2 + \sigma_w^2\,)$$

where $\sigma_{u,v,w}$ refers to the standard deviation of wind speed turbulent fluctuations in the *x, y, z* directions respectively.

3.2. Wetzstein

This mast is located in Germany (50° 27'N, 11° 27'E) and data were available for the period of 12/04/05 – 19/08/05 as 30 min averages. As it was part of the same project as the Norunda site it is also located in the midst of a large coniferous forest. The mean canopy height is 20m and the mast is located on the top of a slight hill. A pair of sonic anemometers (Gill R3) was located at 24m and 32m which again allowed most of the metrics to be calculated. However, data for σ_φ were not available.

No temperature data were available except for values of virtual acoustic temperature as calculated by the sonics. It was found that these data were not of sufficient quality despite application of a correction for the effects of humidity and pressure [12].

Solar irradiance data were again available from measurements made above the canopy. Values for α between 24 m and 32m and *TKE* at 32m were calculated as the metrics of interest for the purposes of resource assessment.

3.3. Sirta

This site is located in the Palaiseau Ecole Polytechnique (48° 42' 50" N , 2° 12' 39" E). The mast is located in a semi-urban area with a large mixed forest located to the north-east at a distance of c. 55m which extends a distance c.560m along a bearing of 37° from the meteorological mast.

The instrumentation is comprised of sonic anemometers (Meter USA-1) and temperature sensors located at 10m and 30m. Additional information on the instrumentation can be found in [13]. Data were available between 04/05/07 – 18/05/09 as 10 min averages. These were filtered to examine directions of between 25°- 47° in order that the effect of the canopy could be assessed.

All stability metrics were again calculated with the exception of σ_φ due to a lack of available data and also Ri_{b2} as it is not applicable outside of a canopy. For comparison purposes, α was calculated between 10m and 30 m and *TKE* was calculated at 30m. Concurrent irradiance data were not available and so annual average data from the Meteonorm database were used [14].

3.4. Vaudeville-le-Haut

This mast is located in a wind farm in France (46° 26' 58"N , 05° 35' 02"E). There is an extensive mixed forest with a mean canopy height of 30m located to the east at a distance of c. 130m. Two operating turbines are located at a bearing of 69° and a distance of 234 m and 23° at a distance of 600m from the mast. Data were available between 01/01/10 – 31/12/11 as 10 min averages from a series of sonic anemometers (Metek USA-1), temperature sensors and wind vanes on a 100m mast [15].

Due to a lack of access to the full data sets, only values for S, σ_φ , Ri and Ri_b have been calculated between heights of 40m and 80m. Values for α were calculated between 60m and 80m along with values for turbulence intensity (*TI*) at 80m defined as:

$$TI = \sigma_u/\overline{U}$$

Unfortunately it was not possible to calculate values of *TKE* as per the other sites.

Analysis was carried out for two direction sectors. One in which the wind will have travelled through the dense forest (*"V- forest"*), 240° - 260°, and the other over flatter terrain (*"V-flat"*) , 30° - 50°. Flow in this second direction sector will have been perturbed by the two turbines mentioned above; however, it will provide some comparison for the effect of the forestry. Solar irradiance data were again provided for the same period from a pyranometer on site.

4. Methodology

The values of *TKE* or *TI* and α as outlined above were considered for each case. The spread in observed values was considerable as can be seen from the scatter plots for Norunda in Figure 2.

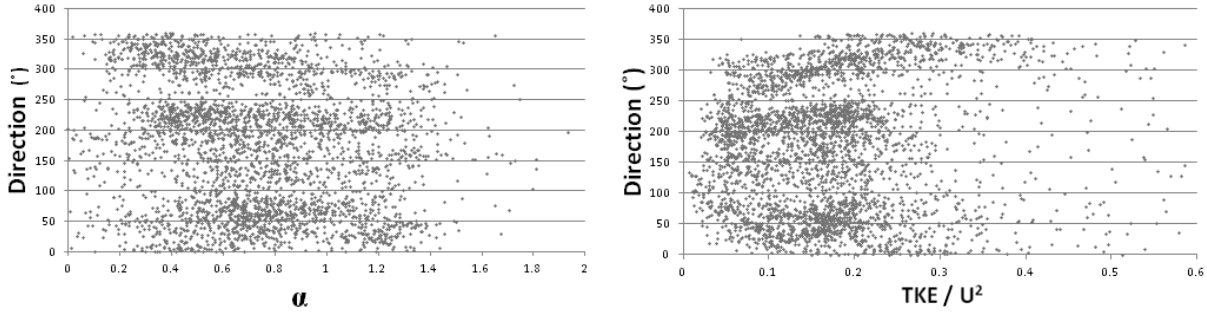

Figure 2: Scatter plots of $\boldsymbol{\alpha}$ and $TKE/\overline{\boldsymbol{U}}^2$ against direction for Norunda.

There are many possible causes of such a spread in values particularly in forested terrain where the drag which the canopy exerts on the flow changes seasonally. In order to identify α and *TKE* values that would be indicative of neutral conditions the Pasquill stability classes were used.

In this method, classes are defined as: A- Unstable, D- Neutral, F-Stable with C, E and B representing intermediate states. Table 1 indicates when such events are expected for certain irradiance levels and mean wind speed, $\overline{U}$, measured at 10m above ground level in flat open terrain [24]. The classification of irradiance level in this system is rather subjective. Attempts have been made to link the categories used by [24] to W/m^2 values or to solar altitude [25]. However, the important factor to note in Table 1 is the sensitivity of the prevailing stability class to the incident irradiance for low wind speeds. This will discussed further below.

Table 1. Pasquill's stability categories

	Irradiance			**Night**	
$\overline{U}$ **(m/s)**	Strong	Moderate	Light	Overcast (>4/8 Cloud)	Cloudless (<3/8 Cloud)
<2	A	A-B	B	-	-
2-3	A-B	B	C	F	F
3-5	B	B-C	C	D	E
5-6	C	C-D	D	D	D
>6	C	D	D	D	D

As we can see from Table 1 above, the prevailing stability conditions are sensitive to irradiance levels at low wind speeds but this relationship is removed for higher wind speeds when neutral conditions prevail. This trend was observed for Norunda as can be seen in Figure 3. Values for *TKE* have been normalised to the square of the mean wind speed for comparison.

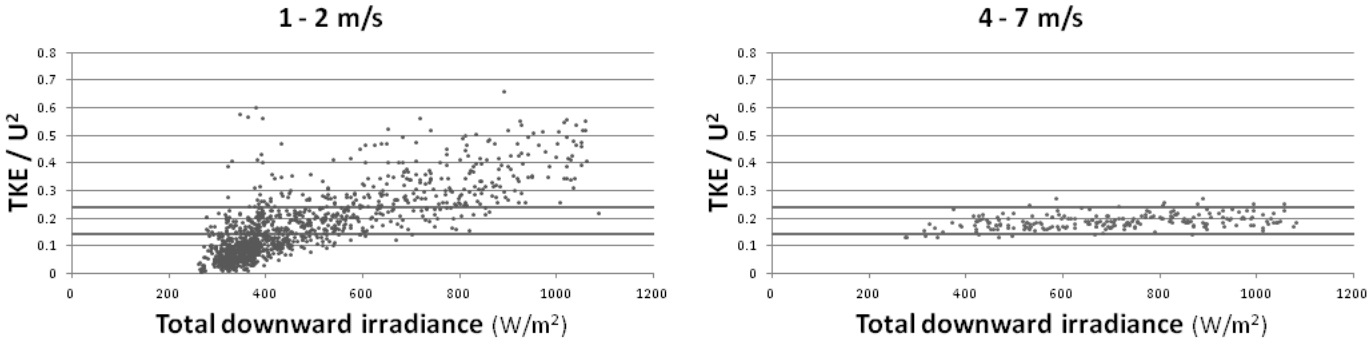

Figure 3: Scatter plots of $TKE/\overline{U}^2$ against irradiance for low and high wind speeds.

The reduced scatter of points at higher wind speeds, the trend of which is insensitive to irradiance levels, suggests that a value of $TKE/\overline{U}^2$ from 0.14 to 0.24 would be expected in neutral conditions. Bars indicating this range are included in Figure 3.

A similar collapse of data was found for both *TKE* and α and for all five cases. Values expected for neutral events for each case are given in Table 2.

Table 2. Expected neutral values

Case	**TKE/U²**	**Alpha**
Norunda	0.14-0.24	0.38-0.71
Wetzstein	0.11-0.17	0.7-0.85
Sirta	0.11-0.16	0.46-0.63
V-forest	0.14-0.23*	0.29-0.53
V-flat	0.14-0.24*	0.32-0.54

* Turbulence intensity.

There were some problems in identifying neutral conditions for α in the case of Sirta. This was due to the fact that two separate mean neutral values exist depending on the season. This was taken to be a consequence of increased foliage during the summer months in the mixed forest. Due to a lack of measurements these points were discarded. This problem was not found in the other cases, a fact likely due to less severe seasonal foliage variations.

A scatter plot of values for α versus $TKE/\overline{U}^2$ was then produced. An example of such a plot is given for the Norunda case in Figure 4.

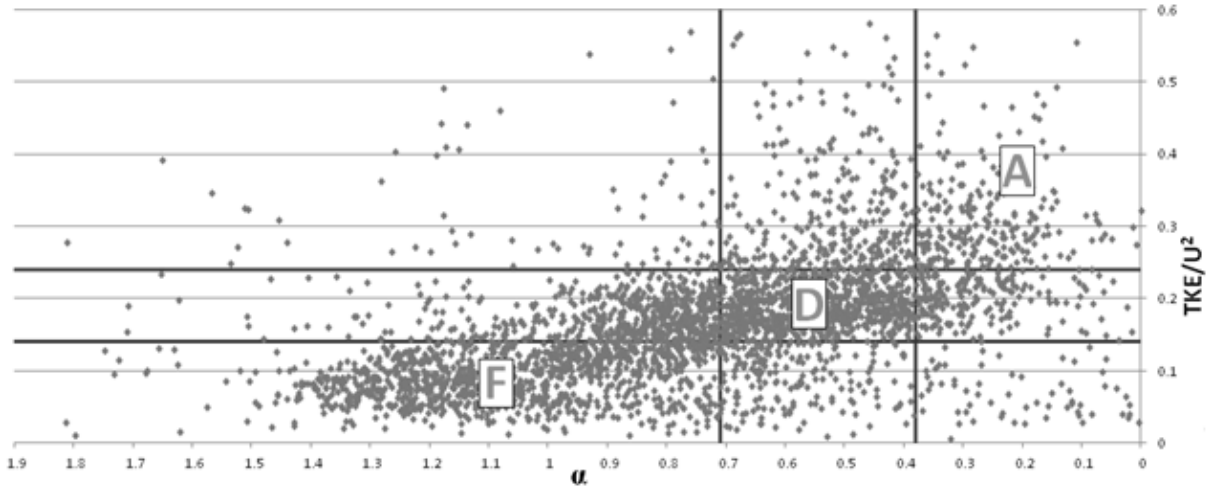

Figure 4: Scatter plot of $TKE/\overline{U}^2$ versus α for the Norunda case.

The included bars, which create nine segments, indicate the neutral ranges of α and $TKE/\overline{U}^2$ as given in Table 2. Segments located on the main diagonal are labelled A,D,F as per the Pasquill classification.

The three labelled segments (the boundaries for which have been determined using the Pasquill stability classes) clearly display characteristics of atmospheric stability of interest to the wind energy industry (e.g. high shear and low turbulence for stable events). Thus, we can say with a degree of certainty that they are indeed F-stable, D-neutral and A-unstable events. The classification of points in the other segments is less certain and so they are disregarded for the purposes of assessing the stability metrics. For the five cases investigated, on average 60% of points were retained following this stage.

The next step was to indentify which stability metric was best able to differentiate between the A-stable, D-neutral and F-unstable categories as identified by the method above. The scatter plots in Figure 5 show the level of this differentiation for Norunda using two of the stability metrics.

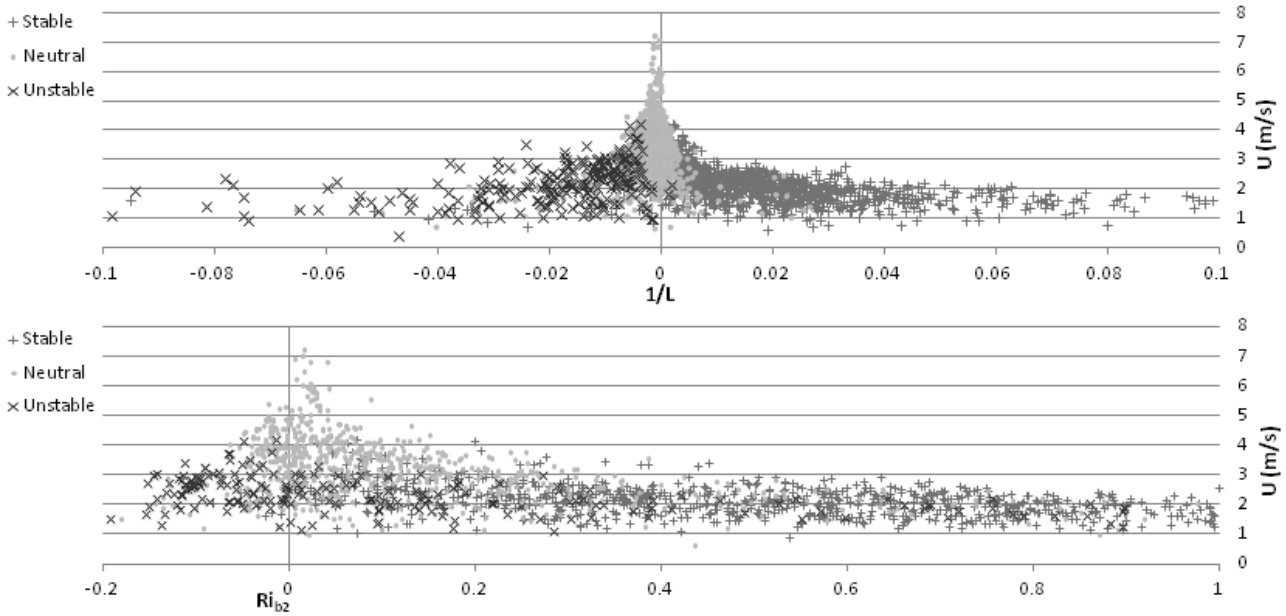

Figure 5: Scatter plots of $1/L$ and Ri_{b2} against wind speed for Norunda.

As can be seen from the scatter plots in Figure 5, differentiation of the stability classes is more successfully achieved using $1/L$ rather than Ri_{b2} for the Norunda case. However, in order to compare all metrics for all cases in a non-subjective manner, it is necessary to devise a measure of the level of differentiation. This was achieved by writing a short program which identifies the line of best fit to segregate stable-neutral and neutral-unstable cases. The program incrementally adjusts the positions of these dividing lines until a position which minimises categorisation error is achieved.

For example, in the Norunda case, these dividing lines were identified as $1/L$ = 0.00198 m^{-1} and $1/L$= -0.00692 m^{-1}. Thus, if a stable point's value of $1/L$ is greater than 0.00198 m^{-1} it is correctly categorised and is counted as a "hit". Using this method, 89% of values were correctly categorised. The corresponding figure for Ri_{b2} was 70%. This indicates that $1/L$ is more successful at identify stability events of interest for this particular case.

Results for all metrics and for all cases are presented in Table 3 which can be found in the appendix. Data points for wind speeds of < 2m/s have been excluded from this analysis as the ability to differentiate stability class is poor at such low wind speeds and they are not relevant for wind energy generation.

5. Discussion

The ability of each metric to differentiate between stability events of interest is discussed below.

5.1. Obukhov & Kazanski-Monin

The Obukhov length was the best performing metric for each case in which it could be calculated. The threshold values for neutral events are relatively consistent for each case, and are of the same order of magnitude of the expected values quoted in subsection 2.4.

The superior performance of this metric may be due in part to the fact all measurements are performed by a single instrument, i.e. a sonic anemometer, which has a high level of accuracy. This eliminates the inherent potential error in the other metrics which rely on multiple measurement technologies to produce synchronous results.

The Kazanski-Monin parameter performs comparably which would suggest that the Coriolis Effect is not an issue at the heights considered.

5.2. Richardson numbers

The Ri_b outperforms or provides similar results to Ri for each case. This is with the exception of the Wetzstein case where, as discussed in sub-section 3.2, results are befuddled by a lack of reliable temperature data due to the use of sonic anemometry to measure the virtual acoustic temperature.

The performance of the Ri_b for the Norunda and Vaudeville sites is particularly interesting as it is devised as a crude approximation of Ri. This may be due to sensitivity of the Ri to the $(d\overline{U})^2$ term in the denominator which produces unreliable results at low wind speeds or for low wind shear. As mentioned above, there is also inherent error in relying on up to four instruments to provide high quality synchronous data.

Furthermore, it may be difficult to establish a sensible gradient of mean wind speed or indeed temperature in complex sites with turbulent flow. Comparing values for Ri and Ri_b in V-flat against V-forest would suggest that the metrics are more applicable in simpler terrain where the flow is less turbulent and meaningful averages of U and θ are more likely to exist.

The results for Wetzstein highlight the need for accurate temperature measurements. Although this is not an issue for modern instrumentation it may be a problem when converting recorded temperatures to potential temperature values. This conversion depends on ambient humidity and pressure levels which introduces dependence on more instrumentation and hence increases potential error. In this paper we have used the dry adiabatic lapse rate of -0.0098 K/m for all conversions [6]. It appears that the use of the virtual acoustic temperature has not adversely affected calculation of the Obukhov length. This is likely due to the fact that the calculation of this metric requires parameterisation of the fluctuations observed in temperature measurements rather than absolute values.

Results achieved using Ri_{b2} are poor which is disappointing as, in [8], this metric proved successful in identifying stability effects within five forest canopies in complex terrain. This disparity is likely due to the fact that the cited research is in the area of CO_2 fluxes and so is focused on flow parameters and effects of stability which may not be directly relevant to the wind energy industry.

5.3. Environmental Stability Parameter

This parameter produces results comparable to Ri and Rib. The quality of results is again reduced in more complex sites as can be seen from comparing results from the two Vaudeville-le-Haut cases and the flat Norunda against the hilly Wetzstein. This may be due to the lack of meaningful average values of θ in more complex terrain as discussed above, or the increased importance of shearing effects in such sites, which this metric ignores.

It is also important to note that depending on the stratification above the surface layer, the effect of the local gradient in potential temperature may be insufficient to determine the full stability characteristics of the atmospheric boundary layer. This would require measurements of temperature at greater heights than are commonly achievable using a standard meteorological mast. This is explained by the series of graphs on p. 170 of [6] to which the reader is referred.

5.4. Standard deviation of direction

This metric performs surprisingly well given the fact that it is by far the easiest to measure and relies on the reliable and well established technology of the wind vane. However, it is clear that threshold values of $1/\sigma_\varphi$ will not be sufficient for the purposes of resource assessment as they are site, height

and direction sector dependant. Also, such data provide little information as to the structure of the boundary layer for the purposes of simulation.

This metric may perhaps be best used alongside more comprehensive measurements, such as sonic anemometry, so that $1/\sigma_\varphi$ can be correlated to stability categories. This data could then be used in the event of failure or redeployment of the other instrumentation.

6. Implications

In order to gain an appreciation of the likely effect of stability on wind generation the most effective metric for each case was applied to the complete data sets. Wind speeds were scaled up to a realistic hub height of 100 m using the calculated α and the standard power law formula. Although this equation relies on a number of assumptions and may not be reliable in such complex sites, the derived values are more indicative of wind energy potential than those measured a few metres above the canopy.

Data were binned into wind speeds and segmented by percentage occurrence of stability class as shown in Figure 7. A graph showing the number of data points in each wind speed bin is overlaid for information. Results for the Sirta are shown in Figure 6. Although it may be desirable for continuity to display results for Norunda, this is not the best case to consider for the effects of stability on wind energy potential due to the low wind speeds and the fact that it was found to have unusually stable nights [16].

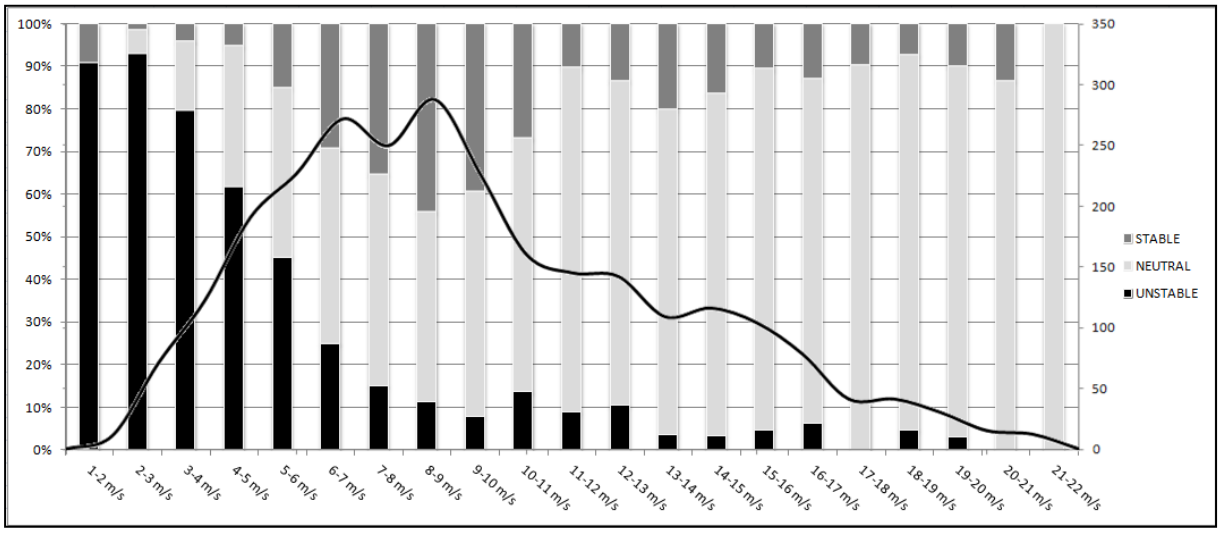

Figure 6: Occurrence of stability events for different wind speeds at the Sirta case. This graph was produced using threshold values of 1/L given in Table 3.

On inspection of Figure 6, and the other graphs in the appendix, it is clear that non neutral stability events are common especially for wind speeds below 10 m/s.

It is also interesting to note that there is only marginal difference in the occurrence of non-neutral events between V-flat and V-forest which may indicate that the presence of forestry has little effect on stability. However it is important to note that although the V-flat direction sectors contain considerably less forestry the entire site is characterised by pockets of trees. Also, flow in this direction sector is likely be perturbed by the operational wind turbines mentioned previously. Unfortunately, unobstructed direction sectors were not available for comparison at the other sites.

It is important to understand how these non-neutral events affect the wind resource. In [17] it was noted that the effects of stability are specifically influential in the development of internal boundary layers in areas of abrupt roughness, temperature and moisture changes. This would indicate that stability effects will be particularly important when modelling the transition from forested to grassland or other less complicated terrain.

It is desirable to quantify the effect that these non-neutral events have on the wind resource due to altered wind shear, levels of turbulence and the persistence of wakes. However, this is difficult to assess the without extensive modelling and so will not be considered here.

There are methods that can be used to approximate the effect of, for example, wind shear on power generation, e.g. the equivalent wind speed for AEP method [18] and the cosine loss model for inflow angle [19]. However, these methods are highly technology dependant as some turbines are now being designed with the ability to adjust their operation to mitigate losses due to such effects [20]

7. Conclusions

It is clear that the Obukhov Length, L, as calculated by a fast response sonic anemometer, provides the most consistent results in identifying non-neutral stability events in the highly complex sites considered.

It is possible to classify approximately 60% of events in the considered cases into stable, neutral and unstable categories by simply analysing data that are measured as standard at potential wind farm sites, such as α and *TKE* or *TI*. An analysis of such data was used in [21] to identify stability events in moderately complex terrain and it would appear from the present paper that a similar approach is also applicable in these highly complex sites.

Although simple metrics do provide information on the effects of stability events they do not provide any information on the cause, such data will be required if realistic simulations are to be conducted. If we are to successfully model non-neutral events in complex terrain we will require information on thermal stratification, vertical heat flux and values for quantities such as U_* in the surface layer. These data will be required to select appropriate boundary conditions and accurately describe buoyancy forces in computational simulations.

Given the performance of the Obukhov length it would appear that these data are best collected with the deployment of 3D sonic anemometry.

8. Acknowledgments

Special thanks to Eric Dupont, Christian Feigenwinter and Oliver Texier for providing access to comprehensive data sets which have allowed the analysis in this paper to be conducted.

This work has been carried out with funding from the EU FP7-PEOPLE program under WAUDIT Marie-Curie Initial Training Network.

9. Appendix

Table 3: Results the analysis of the stability metrics as presented in Section 4.

Site			$1/L$	$\mu(-)$	Ri	Ri_b	Ri_{b2}	S	$1/\sigma_\varphi$
Norunda	Hit % :		**89**	88	80	82	70	83	85
Measured at: 28-36.9m	Stable if :	>	**0.002 m^{-1}**	3.54	0.038	0.006	0.185	0.00025 s^{-2}	0.05$^{-1\circ}$
	Unstable if:	<	**-0.007 m^{-1}**	-14.63	-0.078	-0.008	-0.022	-0.00042 s^{-2}	0.04$^{-1\circ}$
Wetzstein	Hit % :		**91**	**91**	46$^+$	39$^+$	39$^+$	65	-
Measured at: 24-32m	Stable if :	>	**0.003 m^{-1}**	**7.04**	1.47$^+$	0.28$^+$	0.0702$^+$	0.0004 s^{-2}	-
	Unstable if:	<	**-0.004 m^{-1}**	**-9.65**	2.07$^+$	0.135$^+$	0.0337$^+$	-0.00033 s^{-2}	-
Sirta	Hit % :		**79**	77	78	78	-	70	-
Measured at: 10-30m	Stable if :	>	**-0.001 m^{-1}**	2.27	0.023	0.0085	-	0.000019 s^{-2}	-
	Unstable if:	<	**-0.004 m^{-1}**	-10.08	-0.04	-0.0095	-	-0.000017 s^{-2}	-
V-forest	Hit % :		-	-	58	69	-	62	**86**
Measured at: 40-80m	Stable if :	>	-	-	0.0709	0.0159	-	0.000272 s^{-2}	**0.0927$^{-1\circ}$**
	Unstable if:	<	-	-	0.0159	-0.012	-	-0.00012 s^{-2}	**0.064$^{-1\circ}$**
V-flat	Hit % :		-	-	67	77	-	71	**86**
Measured at: 40-80m	Stable if :	>	-	-	0.103	0.021	-	0.0035 s^{-2}	**0.1108$^{-1\circ}$**
	Unstable if:	<	-	-	0.181	-0.014	-	-0.0002 s^{-2}	**0.0700$^{-1\circ}$**

$^+$ *These results are based on unreliable temperature measurements and are provided for comparison purposes only.*
BOLD TEXT *indicates the best performing metric for each case.*

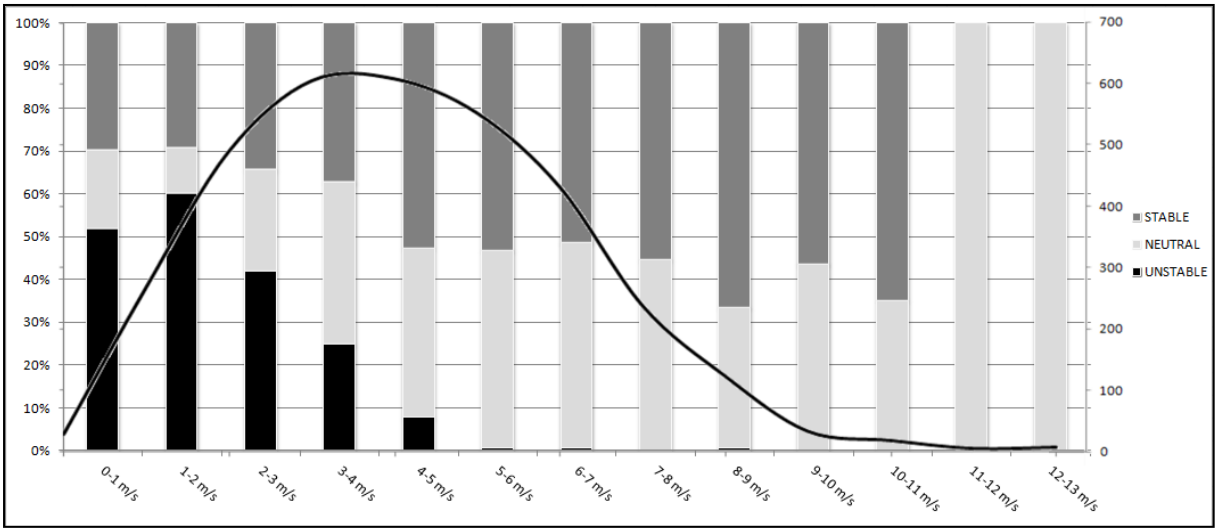

Figure 7: Occurrence of stability events for different wind speeds at Norunda. This graph was produced using threshold values of $1/L$ given in Table 3

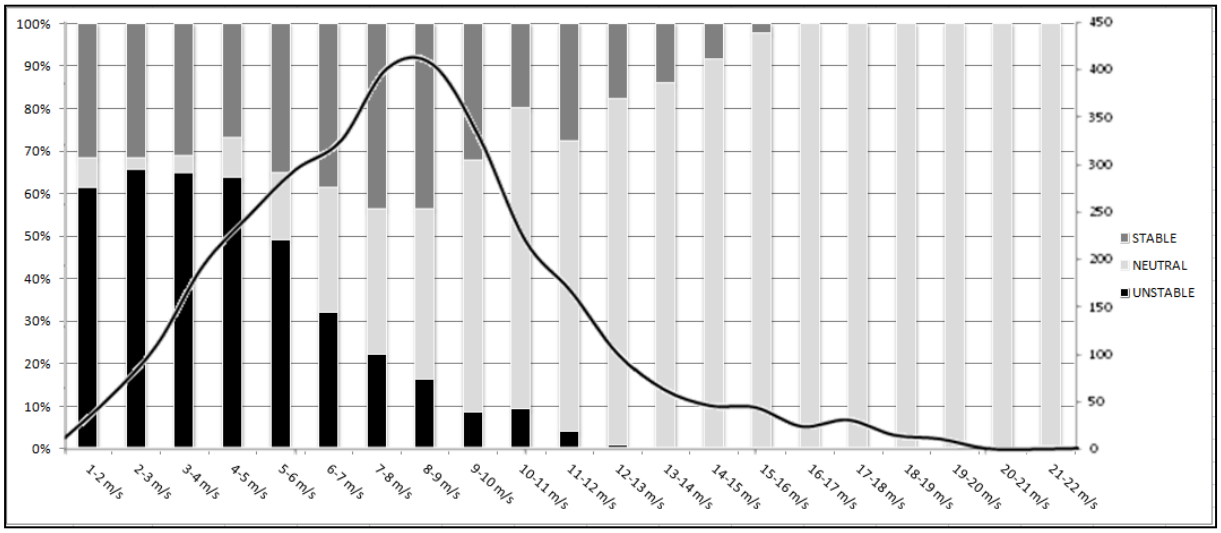

Figure 8: Occurrence of stability events for different wind speeds at the Wetzstein case. This graph was produced using threshold values of $1/L$ given in Table 3.

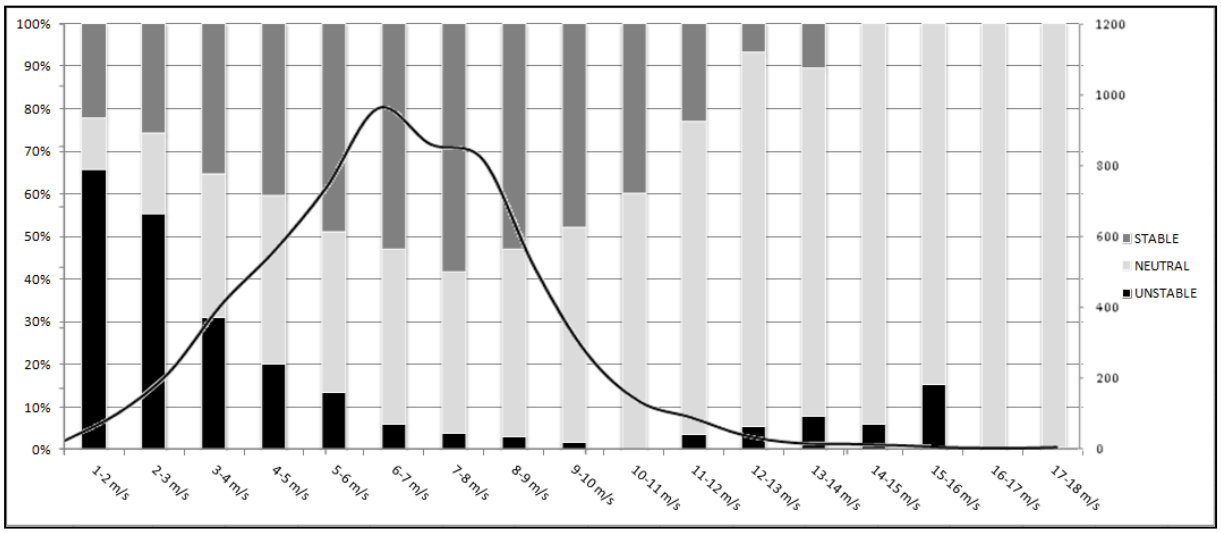

Figure 9: Occurrence of stability events for different wind speeds for the V-forest case. This graph was produced using threshold values of $\boldsymbol{\sigma_{\varphi}}$ given in Table 3.

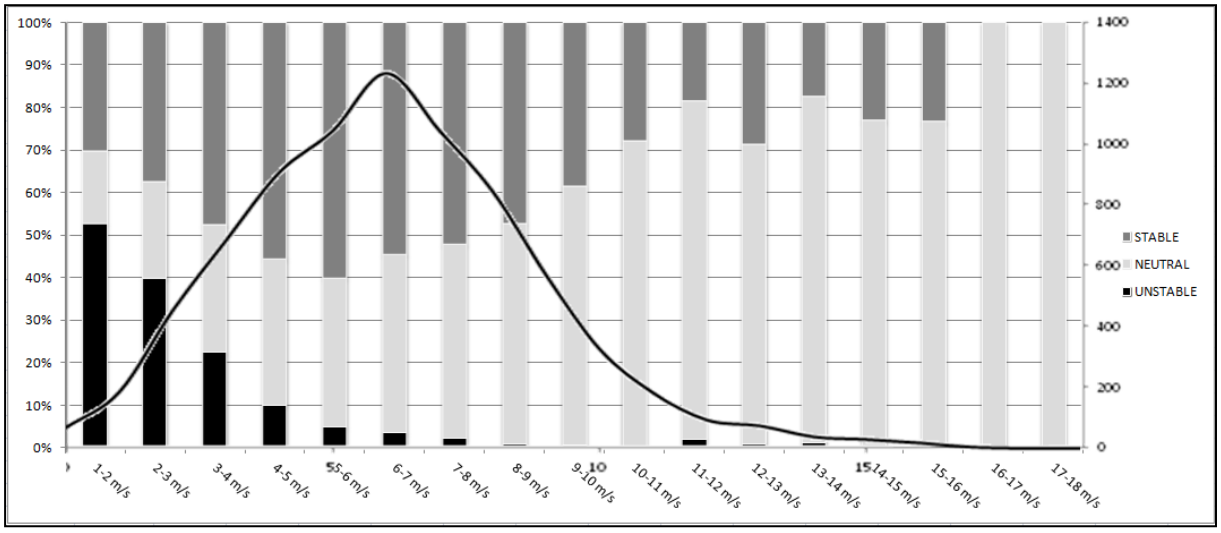

Figure 10: Occurrence of stability events for different wind speeds for the V-flat case. This graph was produced using threshold values of $\boldsymbol{1/\sigma_{\varphi}}$ given in Table 3.

10. References

[1] Belcher S et al. 2012 The Wind in the Willows. Flows in forest canopies in complex terrain *Annual review of Fluid Mechanics* **44** pp 479-504
[2] Kaimal J C and Finnigan J J 1994 *Atmospheric boundary layer flows* (Oxford: University Press)
[3] Wylie S and Watson S 2011 *A CFD study of wind flow around a model forest: Proc. EWEA (Brussels, Belgium, 14-17 March 2011)*
[4] Montavon C 2012 *Modelling Of Wind Speed and Turbulence Intensity For A Forested Site In Complex Terrain: Proc. EWEA 2012 (Copenhagen, Denmark, 16-19 April 2012)*
[5] Desmond C J et al. *Forest canopy flows in non-neutral stability: Proc. EWEA 2012 (Copenhagen, Denmark, 16-19 April 2012)*
[6] Stull R 1988 An *introduction to boundary layer meteorology* (Dordrecht: Kluwer Academic Publishers)
[7] Irwin J and Binkowski F 1981 Estimation of the Monin Obukhov scaling length using on site instrumentation *Atmospheric Environment* **15** 6 pp 1091-1094
[8] Burns S et al. 2011 Atmospheric stability effects on wind fields and scalar mixing within and just above a subalpine forest in sloping terrain *Boundary Layer Meteorology* **138** pp 231-262
[9] Mannan S and Lee F 2005 *Lee's Loss Prevention in the Process Industries* (London: Elsevier)
[10] Office of Nuclear Regulatory Research 2007 *Regulatory guide 1.23: Meteorological monitoring programs for nuclear power plants* (Washington: US Nuclear regulatory Authority)
[11] Feigenwinter C et al. 2008 Comparison of horizontal and vertical advective CO2 fluxes *Agricultural and Forest Meteorology* **148** pp 12-24
[12] Lanzinger E and Langmack H 2005 Measuring air temperature by using an ultrasonic anemometer: *Proc. TECO (Bucharest, Romania, 4-7 May 2005)*
[13] Zaidi H et al. 2011 Evaluating the ability of two canopy models to reproduce the forested area effects using code saturn: *Proc. ICWE 13 (Amsterdam, Netherlands, 10-15 July 2011)*
[14] Meteotest *Meteonorm. Global Meteorological Database Version 7 Software and data for Engineers, Planners and Education* (Bern: Meteonorm)
[15] Texier O et al. 2010 Integration of atmospheric stability in wind power assessment through CFD modeling: *Proc. EWEC 2010 (Warsaw, Poland, 20-23 April 2010)*
[16] Feigenwinter C et al. 2010 Spatiotemporal evolution of CO2 concentration temperature and wind field during stable nights at the Norunda forest site *Agricultural and Forest Meteorology* **150** pp 692-701
[17] Garratt J R 1990 The internal boundary layer. *Boundary Layer Meteorology* **50** pp 171-203
[18] Wagner R et al. 2011 Accounting for the wind speed shear in power performance measurement *Wind Energy* **14** pp 993-1004
[19] Pedersen T et al. 2002 Wind turbine power performance verification in complex terrain and wind farms Risø-R-1330 (Risø: DTU)
[20] Blodau T 2012 How appropriate are sales power curves on complex or forested sites?: *Proc. EWEA Technology Workshop (Lyons, France, 2-3 July 2012)*
[21] Wharton S and Lundquist L 2012 Assessing atmospheric stability and its impacts on rotor disk wind characteristics at an onshore wind *Journal of Wind Energy* **15** pp 525-546
[22] Gryning S E et al. 2007 On the extension of the wind profile over homogeneous terrain beyond the surface boundary layer. *Boundary-Layer Meteorology* **124** pp 251-268
[23] Smith F. B. 1979 The relation between Pasquil stability P and Kazanski-Monin stability u. *Atmospheric Environment* **13** pp 879-881
[24] Pasquill F. 1961 The estimation of the dispersion of windborne material. *The Meteorological Magazine* **90** pp 33-49

[25] Turner D.B. 1970 *Workbook of Atmospheric Dispersion estimates.* (U.S. Department of Health, Education and Welfare)